Journal of Engineering and Technology for Industrial Applications

ISSN ONLINE: 2447-0228

ITEGAM-JETIA

Manaus, v.7 n.30, p. 18-28. Jul/Aug, 2021

DOI: https://doi.org/10.5935/jetia.v7i30.763

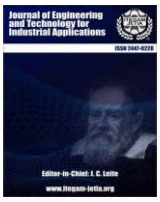

RESEARCH ARTICLE OPEN ACCESS

DISPERSION AND TURBULENCE: A CLOSE RELATIONSHIP UNVEILED BY MEANS OF STATE FUNCTION

Alfredo Jose Constain*[1], Gina Peña Olarte[2] and Carlos Peña Guzman[3]

[1, 2] Fluvia SAS, Bogotá, Colombia.
[3] Environmental and Sanitary Engineering Program, La Salle University, Bogotá, Colombia.

[1] http://orcid.org/0000-0001-6442-0715, [2] http://orcid.org/0000-0002-8727-9088, [3] http://orcid.org/0000-0003-0496-9612

Email: *alfredo.constain@gmail.com, carpeguz@gmail.com, ginap.olarte@fluvia.co

ARTICLE INFO

Article History
Received: July 16th, 2021
Accepted: August 26th, 2021
Published: August 31th, 2021

Keywords:
Turbulence,
Dispersion,
New tracer methods,
New measurement devices.

ABSTRACT

This article reviews the physical conditions that natural, turbulent flows meet to be considered in "Dynamic Equilibrium", a condition that greatly facilitates the analysis of flows, thanks to the concept of "equiprobability", in such a way that the tracer dyes can give an essential information of the dynamics of the current. A general State Function is proposed for this dynamic, which allows to study Advection and Dispersion for virtually all types of river beds, achieving a series of compact and precise relationships, both in hydraulics and thermodynamics. This approach allows us to obviate the limiting use of non-linear differential equations, as "mandatory" characterization of fluid dynamics. With this new method, a practical case from the technical literature is analyzed, and it is solved in detail, comparing it with the classic method of Statistical Moments. Conclusions on results, and recommendations are made.

I. INTRODUCTION

With the worsening of environmental problems, derived from the intense industrialization and expansion of the urban frontier, the availability of powerful methods for the interpretation and study of these issues takes on vital importance.

Paradoxically to this serious situation, since the end of the century, the methods of measurement and study of the phenomena of water pollution practically advanced a little in the theoretical part, and except for the development of increasingly advanced digital platforms, and some new ones. Ideas on how to approach turbulence from *emerging concepts* [1], far from the classical approximation of non-linear differential equations, the methods currently used are practically the same as in the 1990s. For this reason, the renewal of approaches and procedures is an important point from which you can make up for lost time.

With this optics in mind, this Article aims to question some key points about the conceptualization of the dynamics of channels, based on dispersion as a substrate of turbulence, and limited by the relative control of fluctuations (steady state), typical of the "linear" regime of non-equilibrium thermodynamics. A first basic point in this approach is that the energetic conditions are reviewed by which it can be understood why natural, turbulent channels, in "normal" (not catastrophic) conditions, are in a low or moderately strong degree of instability, which allows the entropy production should be at a minimum value, and therefore (according to Boltzmann) present in the system, condition of "Equiprobability", leading to a "statistical constancy" of the average flow velocity.

A second point analyzed is a new Dispersion-Advection model, which basically depends on the mean velocity of the flow and on a "State function" that guides the evolution of the injected tracer cloud, and which, being also a "thermodynamic potential", indicates us when the cloud loses degrees of Freedom, of great significance when we want to calculate the situation of "Complete mixture" for water quality studies.

Turbulence in "steady state" allows the condition of "Equiprobability", which in turn allows a statistically "constant" flow rate. The subsequent dispersion can be defined very precisely.

Finally, a tracer experiment documented in detail in the technical literature is chosen, to which the new model is applied, and the results are compared with the classical Moment methodology.

II. THEORETICAL REFERENCE

Considering the enormous difficulty that has been the deep understanding of turbulence from the Navier-Stokes non-linear differential equations, alternative approaches to the problem have emerged since the end of the last century. One of them, quite different and novel, is Emergent Analysis, in which it is recognized that, in real physical processes, the whole is not the sum of the parts, this since non-linearity and multiple feedbacks in said processes, invalidate the superposition principle, and fill the equations with multiple “incomputable” solutions. It had always been believed, as a fundamental paradigm of science, that starting from the basic processes (at the molecular level, for example) it was possible to describe phenomena of a higher level (at the human level) as “synthesis” of those previous levels. This is not possible due that “the analysis abandons us”, in line with Euler's prophetic words. As each level of reality demands its own calculation rules, it is necessary then, to formulate “emergent” approaches that cover those levels.

An analysis in this line of thought is to define the conditions in which the turbulence remains stable or not, at room temperature, without going of course to the complete analysis from the origin, via Navier-Stokes, which can be done from the thermodynamics of irreversible phenomena. From these results, anticipated by J. Frenkel in the last century, certain important conclusions can be drawn to give a useful interpretation to river hydraulics, especially considering the application of dye tracers.

II.1 REGIMES OF CONTEMPORARY THERMODYNAMICS

Depending on the intensity of the flow of energy or substance (entering or leaving) in open real systems, its state can be placed in one of the thermodynamic stages according to the following classification [2]:

A - Strict equilibrium, corresponding to totally reversible processes, in which causes, and effects disappear, in response to the statistical homogeneity of the parameters associated with this state. Thus, the “Thermodynamic forces”, **F**, (temperature, concentration, free energy gradients, etc.), and their consequences, the “Thermodynamic flows”, **J**, (rates of heat transport, free energy, etc.), they are completely canceled. The fluctuations disappear quickly by the physicochemical control mechanisms. And it is proper to define “thermodynamic potentials” that allows establishing criteria for evolution towards maximums or minimums. For example, in this case, the Entropy Production, σ, null.

B - Quasi-equilibrium, or Linear Irreversibility close to equilibrium, in which the forces and thermodynamic flows are not zero, but are proportional to each other, for this reason, this stage is called “linear”, close to equilibrium. Likewise, fluctuations do not disappear completely, but they are an important aspect of instabilities, without producing catastrophic effects. In this case, when the Forces and Thermodynamic Flows are proportional to each other, the Entropy Production is set at a *minimum* value, according to a famous theorem of I, Prigogine [3]. According to the probabilistic concept of L. Boltzmann [4], a maximum entropy in a system implies that the probabilities at each point are equal [5], which is called as the “Equiprobability” condition. If the entropy according to Boltzmann is:

$$\sum_i Log\ p_i \sim Maximo \tag{1}$$

This implies that:

$$p1 + p2 + p3 + \cdots + pn \approx 1.0 \tag{2}$$

And that:

$$p1 = p2 = p3 = \cdots = pn \tag{3}$$

In other words, for a maximum entropy, the probabilities at each point in the system are equal. Now, for this maximum condition, the entropy production is a Minimum.

$$S \to Max,\ \ \sigma \to Min \tag{4}$$

C -Dissipative Non-Equilibrium, or distant Irreversibility, a state in which there is no proportionality between Forces and Flows and their relationship is non-linear, which is why this phase is precisely called “non-linear”. The production of entropy grows and is no longer a minimum, and the fluctuations grow to levels close to the average value of their set. In this extreme state, new structures appear in matter, combining order and disorder.

II.2 PROBABILISTIC DISTRIBUTIONS AS A SUITABLE DESCRIPTION OF NATURAL PROCESSES

The vision of irreversible molecular phenomena has focused primarily on the “Probabilistic distributions”, or Gibbs statistical entities [6], defined as follows, for a case “j” (of “n”) possible:

$$\rho_j = \rho(p_j, q_{j\,,} t_j) \tag{5}$$

This value indicates the probability of finding the values of linear momentum, **p**, and coordinates, **q**, at time, **t**. In practice this Distribution indicates the density of points in a certain finite region of the phase space. Figure 1.

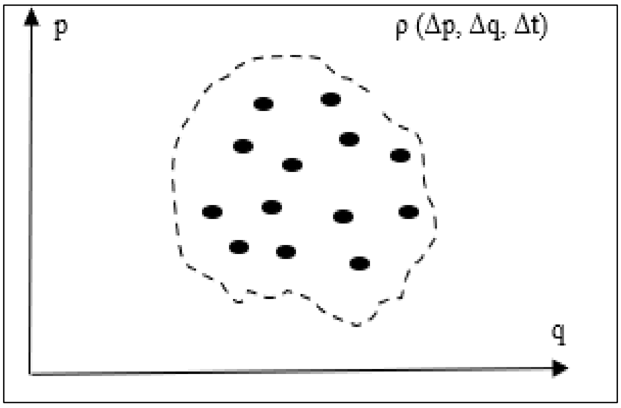

Figure 1: Probabilistic distribution in a physical system.
Source: Authors, (2021).

Unlike the original conception of Gibbs and Einstein, in which the Probabilistic Distributions were fundamentally due to our ignorance regarding the inaccessible massive phenomena of the micro world, the modern view assigns them a much more fundamental role, as only coherent models of the dynamics at that level, since the “trajectories” have disappeared as their basic description, since they are “divergent” by the “Poincaré resonances” on their coupled modes for the innumerable degrees of freedom. Therefore, they are dynamic entities, inherently non-deterministic, that replace the “trajectories” of the particles, which are essentially “incomputable”, since in irreversible material assemblages, the Fourier spectral harmonic interferences, due to the couplings between the multiple “Degrees of Freedom” lead to dividers that cancel out, giving divergence effects, which destroy these trajectories [6].

Now, for stages A-Strict Equilibrium and B - Linear Quasi-equilibrium, the compliance with the “Equiprobability” condition is of course different in each case, since only in the second case there is irreversible heat generation, increasing velocity fluctuations to a significant level. If the effect of these fluctuations is assimilated to an “absolute error” [7], which affects the value of the distribution, it can then be written for both cases:

$$\rho(A) \approx < \rho_A > \pm\varepsilon_A \tag{6}$$

And

$$\rho(B) \approx < \rho_B > \pm\varepsilon_B \tag{7}$$

Therefore, // εA // <// εB //, and the degree of inequality between these two values, will correspond to the relative deviation of the “Equiprobability” condition for the system.

Thus, by way of simplified comparison, Figure 2 shows three significant cases of flow: A) Strict equilibrium, B) “Linear” quasi-equilibrium, and C). Far from Equilibrium.

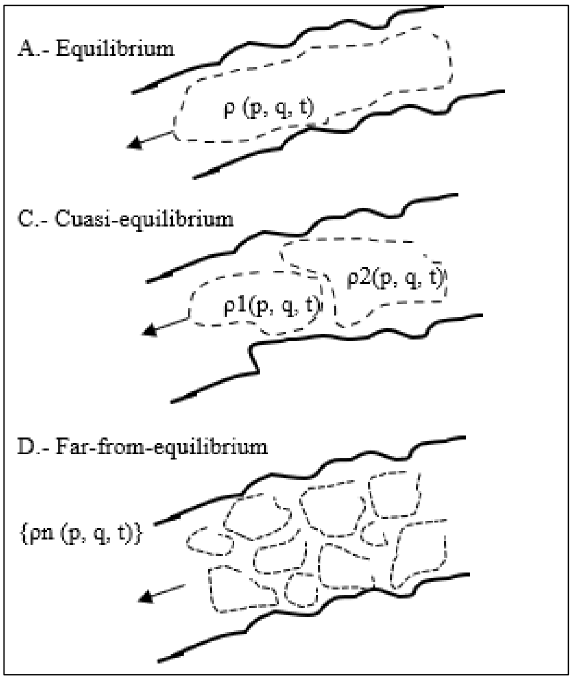

Figure 2: Diferent type of thermodynamic flows.
Source: Authors, (2021).

In A, there is only one Probabilistic Distribution compatible with the strict Boltzmann Equivalence. In B, there are only a very few distributions. In C, there are many distributions, numbered according with “n”. The relative error increases depending on the case, from A to C.

II.3 NATURAL WAYS AS OPEN SYSTEMS EVOLVING UNDER CONDITION OF “DYNAMIC EQUILIBRIUM

Since the “Stable State” corresponding to the irreversible, “Linear” thermodynamic stage, close to equilibrium, is important for the fluvial dynamics under usual conditions, it is necessary to establish the physical conditions that make this stage possible.

For chemical reactions, strict thermodynamic equilibrium requires that microscopic reversibility be fully met, that is, that there is a “Detailed Balance” between contrary reactions. This condition is fulfilled when the cause of the flows, the Gibbs free energy, which in this case is defined as “Affinity”, **A**, is zero. In the regime close to equilibrium, for a mole of substance, this condition is slightly modified as follows:

$$\left(\frac{A}{RT}\right) \ll 1 \tag{8}$$

Here R≈8.31 J/(K * Mol) is the gas constant and T is the Kelvin temperature, which for the usual cases is taken as 300 K. Therefore, the thermal molecular energy is approximately 2.5 KJoules/mol. In most chemical reactions, the molar energies involved are in the range of 10-100 KJ/mol, that is, they do not meet the "linearity" condition of expression (6), and it can be said that these types of effects, at usual temperatures, are in the non-linear regime of irreversible thermodynamics [8].

For the mechanical effects present in natural flows, the criterion of “thermodynamic linearity” must be expressed differently. If the velocity fluctuations in the fluids that make up these flows are small, it is presumable that the instabilities do not lead the turbulent system to a situation of “runaway”, which would be the way in which the system loses its stability. What is the main factor for the water to remain as “still” as possible in the presence of dynamic instabilities? This factor is undoubtedly the “fluidity” of the liquid [9], which is precisely the property of not resisting shear stress. The more “fluid” a liquid is, the more easily it will dampen the fluctuations that occur within it, and the more difficult it will be for it to move out of the “stable state” in which it is close to equilibrium.

According to the liquid model developed by J. Frenkel in socialist Russia in the 1920s and 1930s, the liquid state under normal conditions resembles crystalline solids much more than gases, as is usually the case. it is assumed. The difference between one and the other is more one of degree than of essence, the crystals being much more ordered, especially in the “long range”, where the liquids no longer present any “three-dimensional lattice” characteristics. It is therefore important to numerically characterize the “Fluidity” property from a physical-molecular point of view.

Fluidity can be defined (according to Frenkel) as the situation in which the molecules of the liquid vibrate occupying transient equilibrium positions in their quasi-crystalline lattice, jumping from time to time to a new empty neighboring position, called “hole”. For this reason, liquid molecules yield much more easily to tangential stresses, reducing external disturbances. The molecules of crystalline solids for their part remain vibrating in these equilibrium positions, much longer, almost permanently, that is, their “half-life time at equilibrium point”, called **τ**, is much greater than the of the liquid. Figure 3.

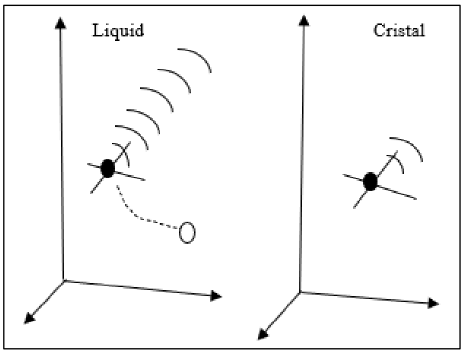

Figure 3: Mechanism of Fluidity in liquids and crystalline solids.
Source: Authors, (2021).

It has been established that this "Half-life time" in equilibrium position" for quasi-crystalline liquids and solid crystals has the following molar shape, as a function of the value of the inherent period of molecular vibration, $\tau o \approx 10^{-13}$ sec:

$$\tau \approx \tau_o\, e^{\frac{W}{RT}} \tag{9}$$

The difference between crystalline solids and quasi-crystalline liquids (for the same ambient temperature) is of course the value of the potential energy, W, called "activation energy". For water, in a range from 300 ° K to 800 ° K, this energy per mole is between 0.57 KJ/mol, and 2.40 KJ/Mol. For crystalline solids under similar conditions, the range of this energy is between 4.8 KJ/mol and 14.4 KJ/Mol. That is, 9 times greater than for water.

It can then be said that, at room temperature (300 ° K), the water meets the following "linear" thermodynamic stability criterion:

$$\left(\frac{W}{RT}\right) \approx \left(\frac{0.57}{2.50}\right) \approx 0.23 \tag{10}$$

Namely:

$$\left(\frac{W}{RT}\right) < 1.0 \tag{11}$$

Therefore, turbulent water partially meets the numerical criterion, not as strict as in expression (8) but allowing a relatively good control of fluctuations due to a significant Fluidity effect. Turbulent water is therefore between the "linear" zone and a catastrophic zone in which this property cannot prevent runaway.

According to equations (6) and (7) in different channels there will be different errors, but it will be possible to apply without fear the concept of "Equiprobability", and consider the statistical constancy of its dynamic parameters

One way to really appreciate what is the meaning of the value expressed in equation (11) is to calculate and compare different values for equation (9) that describes the "mobility" of the water molecules from their equilibrium sites, for several cases significant of the ratio (W/RT):

A - *W/RT≈0.023*

$$e^{0.023} \approx 1.023 \tag{12}$$

B - *W/T≈ 0.23*

$$e^{0.23} \approx 1.26 \tag{13}$$

C - *W/T≈ 2.3*

$$e^{2.3} \approx 9.97 \tag{14}$$

It is seen that the time ratio (τ / τo) varies approximately between 1.02, 1.3 and 10.0, that is, that this ratio for the conditions (W/RT) ≈0.01 and (W/RT) ≈0.23, changes only 23% and it remains well within the same order, close to unity, justifying the great "mobility" of the water molecules at room temperature, and its facility to dampen turbulent fluctuations, to the extent that (W/RT) decreases. Figure 4.

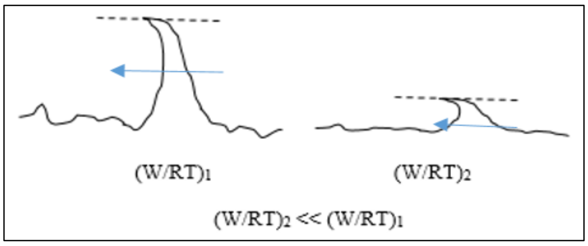

Figure 4: Control of turbulent fluctuations by means of the ratio (W/RT).
Source: Authors, (2021).

II.4 EQUIPROBABILITY CONDITION IN THE NATURAL WAYS AND STATISTICAL CONSTANCE OF DYNAMIC PARAMETERS IN "DYNAMIC EQUILIBRIUM"

Based on what was explained in the previous Section, and considering numerous experimental results, the researchers of river hydraulics have warned that, under "normal" conditions (not catastrophic), natural channels evolve as open systems, (exchanging energy and substance with its environment), within the thermodynamic regime of "Quasi-equilibrium", or of "linear" irreversibility. Therefore, the "Dynamic Equilibrium" or "Stable State" will be the thermodynamic regime that is chosen to analyze its physical dynamics, regarding the contemporary study of turbulence [10][11].

The condition of "Equiprobability" in natural channels can be translated as a situation of constancy of the mass transport rate since this transfer from one point to another will be between points of equal dynamic probability. In Figure 5 the local mass transfers are shown as red paths.

The global (integral) result of these local mass transfers, between equiprobable points, entails the constancy of the mean flow velocity [12]. This speed coincides with the value that defines the Chezy-Manning equation, since the tracer absorbs and expels heat from friction processes in the flow, with "n" as Roughness, R, as Hydraulic Radius, and S, as Longitudinal slope.

$$U \approx \frac{R^{\frac{2}{3}}}{n}\sqrt{S} \tag{15}$$

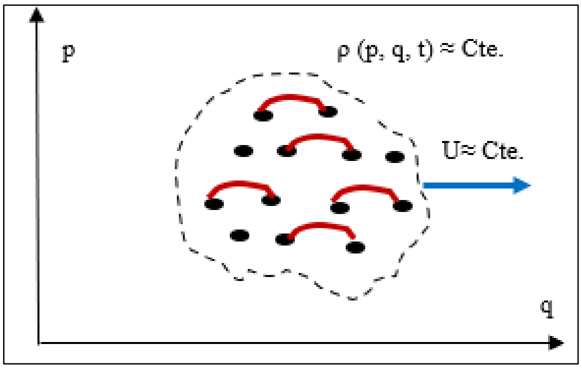

Figure 5: Statistical constancy of mass transfer.
Source: Authors, (2021).

II.5 TRACERS AND THEIR DYNAMICS IN A TURBULENT FLOW

The tracers are inks with special properties that are poured into natural flows to measure and interpret the flow parameters, injecting a certain mass at a point "upstream" of the channel, and measuring the cloud or "plume" of the solute, passing through the "downstream" monitoring point. Once injected into the flow, the mass of the tracer substance is mixed by the effect of turbulence and shear forces that depend on the average flow velocity.

The dynamics of the tracer pen is therefore consistent with the Law of Conservation of Energy, that is, it is a "non-localized" measurement, unlike other measurement methods (such as the Pinwheel or the ultrasound profiler). They operate by means of the Law of Conservation of Momentum and are therefore a more restricted measure of the "local" type. From this perspective, the density of information provided by tracers is important since it depends on a broad set of laws that condition advection and dispersion in natural flows.

The dye tracer substance used must have certain characteristics, such as: **A** - Be soluble in water, **B** - Be environmentally neutral, **C** - Have a physicochemical characteristic that allows it to be detected (measured) by an instrument, **D** - Have a cost compatible with the amounts to be used, and E. - Have a simple protocol for handling and interpretation of the substance and the technology to measure it. Figures 6, 7 and 8.

Figure 6: Rhodamine WT as a fluorescent dye substance.
Source: Authors, (2021).

Figure 7: Fluorometric tracer advancing in a river.
Source: Authors, (2021).

Figure 8: Tracer Measurement "real-time" Instrument.
Source: Authors, (2021).

The tracer ink that is usually used in field experiments is Rhodamine WT (RWT), which is fluorescent, and therefore can be detected with a special optical sensor. The equipment shown measures RWT and common salt in "real time", saving field tasks in memory, or transmitting them over the internet to the cloud.

Modern tracer technologies and methodologies allow accurate and fast measurements even in large rivers. From the information contained in the flared curve (Fickian Curve) that results from the measurement, with convenient values of mass, M, and cross-sectional area *A*. Co is the background concentration of the flow, and E is the longitudinal coefficient of dispersion:

$$C(t,X) \approx \frac{M}{A\sqrt{4\pi E\, t}}\, e^{-\frac{(Xo-U*t)^2}{4\,E\,t}} + Co \qquad (16)$$

Experimenters in the 1960s and after found that the actual tracer curves had a "bias" that was not consistent with the equation above. This bias was significant at the beginning of injection to flow and decreases over time. Co is the basic concentration of the tracer in the flow. Figure 9.

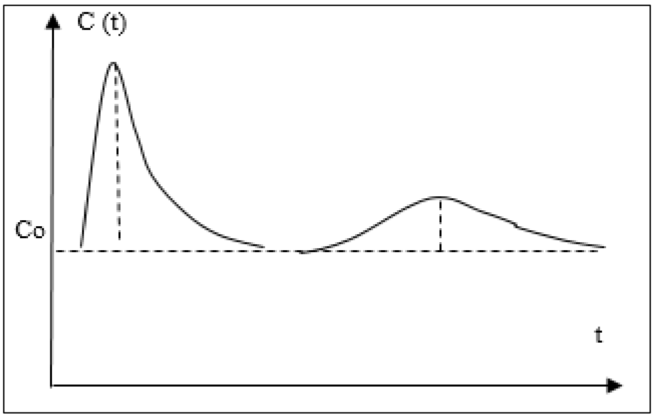

Figure 9: Characteristic Fickiana curve of a tracer.
Source: Authors, (2021).

The bias is a deformation of its symmetry, showing an extended "tail", the explanation of which has taken over a good number of theories of all kinds, but without providing a complete justification that satisfies everyone.

A successful theory to describe this variable bias has been formulated by the authors [13][14], insofar as it provides appropriate quantitative answers to various questions, without having to resort to "Ad-hoc" formulations, such as some of the most common models [15] [16]. This new theory is based on the definition of a State Function, Φ (U, E, t), which describes the thermodynamic evolution of the tracer plume in turbulent flow. This function depends on the mean flow velocity, U, of the Longitudinal Dispersion Coefficient, E, of the Feingenbaum Constant, δ≈4. 6692, and of time, t.

$$\Phi \approx \frac{1}{U}\sqrt{\frac{2*E*\delta}{t}} \qquad (17)$$

It should be noted that clearing the average velocity; U, from the previous equation, there remains a second-order algebraic definition of a formal nature like the Chezy-Manning equation. The classical expression, equation (15), is a function of mechanical forces, while the new equation (18), is a function of electrochemical forces.

$$U \approx \frac{1}{\Phi}\sqrt{\frac{2*E*\delta}{t}} \qquad (18)$$

The magnitudes U, E, and t are state parameters, and therefore the Schwartz condition is satisfied:

$$\oint d\Phi(U,E,t) = 0 \qquad (19)$$

Notable values of the state function are: (tp, 2.16) and (to, 0.38), corresponding to the concentration peak, tp, and now when the tracer loses the transverse degree of freedom, to, and homogeneously fills the cross section of the stream tube through which the tracer advances ("Complete Mix" Condition). Figures 10 and 11.

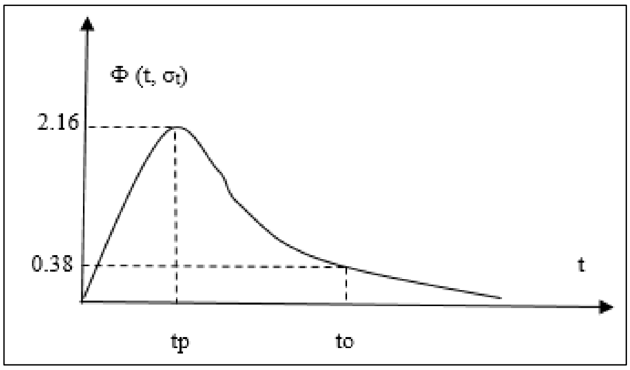

Figure 10: Graph of Φ (U, E, t) at notable times.
Source: Authors, (2021).

The State Function, Φ(t), in its evolution, describes the loss of "Degrees of freedom" of the system, but it also corresponds to the decrease of "Free Energy" in that system.

It must be remembered that when a tracer is injected into the turbulent flow, this mass carries a certain "Energy of formation", which is a potential energy that can be transformed into useful work.

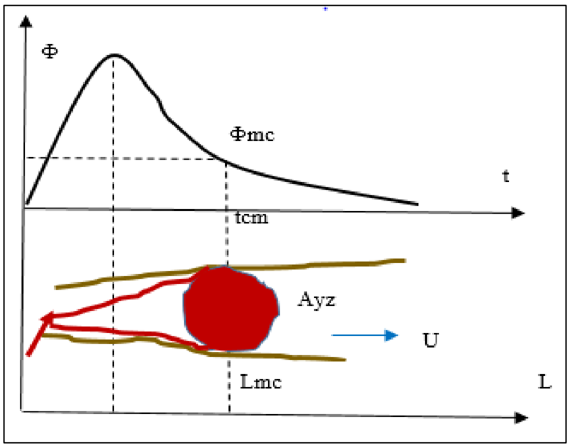

Figure 11: "Complete Mix" condition in flow cross section.
Source: Authors, (2021).

This "Free Energy", G, is gradually used up as the tracer plume advances, generating heat due to the irreversible friction processes in the liquid. Likewise, the principle of entropy increase must be met, and the consequent decrease in entropy production, σ, which tends to a minimum value, when the tracer pen has vanished, and the system is thermodynamically connected with its environment, in the "Dynamic Equilibrium". Figure 12.

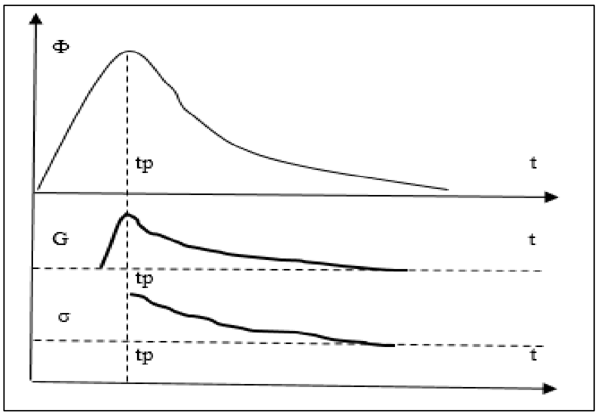

Figure 12: Correspondence between Φ and G and σ.
Source: Authors, (2021).

The state function, Φ(t), then describes the transition between the "pure" dispersion, at the beginning of the injection of the tracer, until the moment of thermodiamic coupling, when there is "pure" turbulence.

A somewhat general model of this "tracer-turbulence coupling", in condition of Dynamic equilibrium of the flow, can be made from the thermodynamic analysis of the tracer plume, from the instant of injection:

$$G = H - T * S \tag{20}$$

Where H is the so-called enthalpy of formation of the tracer solute (constant value depending on the type of substance and its mass), and G is the Gibbs Free Energy, which decreases as the entropy increases. It must be understood that the tracer plume itself, when evolving in the turbulent flow, does not differ essentially from its environment, except for containing that decreasing Free Energy. Figure 13.

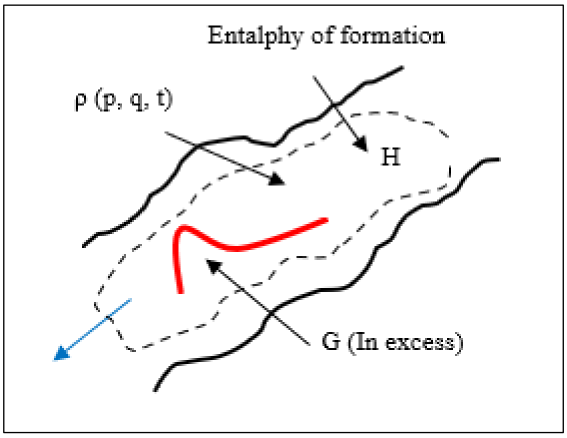

Figure 13: Tracer plume evolving on turbulent flow with an excess of free energy.
Source: Authors, (2021).

In the previous figure, under the condition of a linear "steady state" in the flow, Equiprobability entails a single probabilistic distribution, to which the tracer plume is quite close, until it is completely integrated with its environment, and participates exactly in all its thermodynamic characteristics.

On the other hand, entropy, S, and entropy production, σ, are inverse values, while the former increases monotonically to a maximum value, the latter gradually decreases to a minimum value. Figure 14.

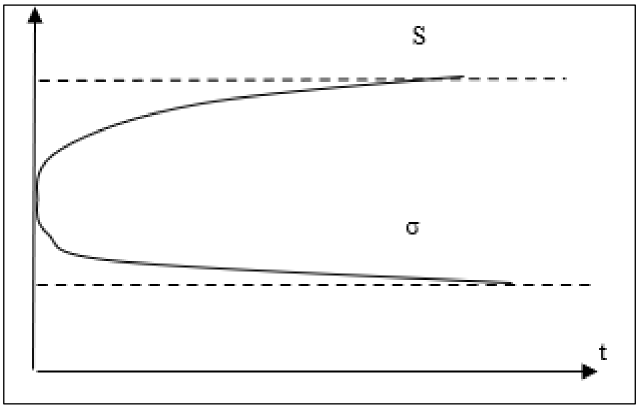

Figure 14: Relationship between Entropy and Entropy production in a linear system.
Source: Authors, (2021).

Therefore, if “a” is a constant of proportionality, it can be established approximately that:

$$S(t) \approx \frac{a}{\sigma(t)} \tag{21}$$

On the other hand, both the state function, Φ (t) and the free energy, decrease monotonically, and it can be said that they are proportional, by means of the constant “b”:

$$G(t) \approx b * \Phi(t) \tag{22}$$

Then, equation (20) becomes:

$$b * \Phi(t) \approx H - T * \left(\frac{a}{\sigma(t)}\right) \tag{23}$$

From this equation in general, it can be verified that the State Function and the Entropy Production are related.

II.6 A NEW MODEL OF TRACER EVOLUTION IN A TURBULENT FLOW

Starting from the classic Fick equation, clearing the value of the Coefficient E, from equation (18) and replacing it in the classic Fick equation, equation (16), with Q, as discharge, it holds:

$$C(t,X) \approx \frac{M}{Q*\Phi*t*1.16}\, e^{-\frac{(t_v - t)^2}{\left(\frac{2}{\delta}\right)*(\Phi*t)^2}} + Co \tag{24}$$

It is useful with respect to the previous equation, to define a “dilution factor” corresponding to the decrease of the peak concentration (the first factor of the right limb) with time.

$$Cp \approx \frac{M}{Q*\Phi*t*1.16} \tag{25}$$

The subsequent analysis of the basic equation of the State Function, Φ(t), equation (17), the following expression can be established, which relates Φ with σt (standard deviation in time), and with tp, the time of the peak*:*

$$\Phi \approx 2.16\left(\frac{\sigma_t}{tp}\right) \tag{26}$$

An important characteristic of the State Function Application Method is that its computations are made based on the Peak Time, tp, and not based on the “Centroid Time”, ts, as is the case with most of current methods. As is known, this time corresponds to the center of gravity of a physical system, that is, where the center of mass is located. Figure 15.

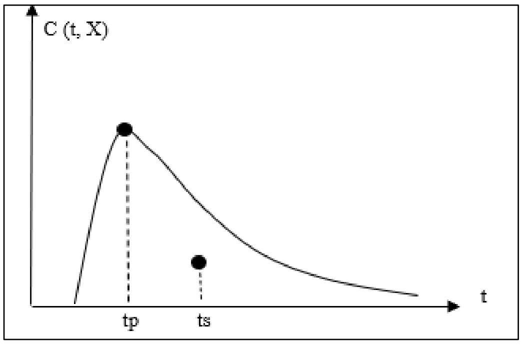

Figure 15: Peak time, and Centroid time.
Source: Authors, (2021).

Now, although apparently this value has a remarkable physical significance for a dynamic system, it has the problem that, in general, there is only one statistical formula for its calculation, which makes it difficult to use in practice. A detailed analysis of this parameter indicates that the difference between the Peak Time and the Centroid Time decreases as the tracer pen advances, indicating that in a certain way this concept reflects that the bias of the curve Fickiana is eliminated at the end, so that she can actively join the dispersal [17].

This non-availability of mass is maintained in practice until the moment in which the tracer homogeneously covers the cross section of the stream tube through which the pen advances, that is, when the State function is equal to Φ≈0.38, as shown in Figure 10. In this case the Centroid Time is only 13% greater than the Peak Time.

Now, with the remarkable values of the curve in Figure 6, it is possible to draw the two approximate real Fickiana curves, with different data, as shown in Figure 16.

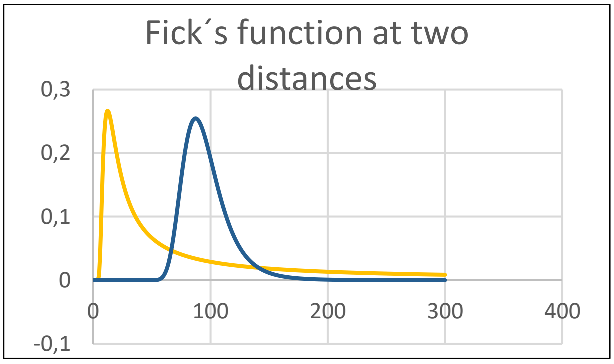

Figure 16: Tracer curves with different skew.
Source: Authors, (2021).

Two important aspects should be noted: A - The bias of the first curve is much more accentuated than that of the second curve, and B.- That the concentration of the second curve is slightly lower than that of the first, as expected since the mass of the tracer is expanding.

The initial curve (yellow) corresponds to the immediate injection point, when Φ≈2.16, its maximum value, here it is fulfilled that σt1≈tp1; the second curve (blue) corresponds to a further point, when Φ≈0.382, the value for "Complete Mix" on the flow cross section.

The reason for the decreasing bias in the tracer Fickian curves is that the state function, Φ(t), decreases with time, and suppressing sequentially degrees of freedom in the system, releasing mass from its initial cohesive volume. Simultaneously the free energy of the tracer is spent, and the production of entropy is tending to a minimum. In this way, the tracer is coupling with its environment, which is in a "stable state" condition of the thermodynamic linear region.

III. APPLICATION TO AN EXPERIMENTAL CASE: COOPER CREECK, VA. USA (1963)

To apply and adjust various river measurement methodologies in the 1950s, the United States Geological Survey (USGS) performed tracer measurements at selected sites, including the Cooper Creeck River near Gage City, Virginia. The river flow when the measurements were made (1959) was in a range of 10 to 15 m3/s [18].

To analyze the data from this experiment, Godfrey & Frederick made an initial analysis of the field data, and Thackston, Hays & Krenkel then carried out a detailed analysis of the possible theoretical alternatives to calculate the Longitudinal Coefficient of Dispersion, since the curves obtained experimentally, they showed some bias (of the Pearson-III type), and the conventional methods of the time did not allow adequate accuracy. For this reason, it was preferred to use the Moments method, which does not recognize the so-called "convective period" (recognized by most other methods), which prevented its application in the early phase of the tracer's evolution. This method only requires that the velocity be approximately constant [19].

To apply and adjust various river measurement methodologies in the 1950s, the United States Geological Survey (USGS) performed tracer measurements at selected sites, including the Cooper Creeck River near Gage City, Virginia. The river flow when the measurements were made (1959) was in a range of 10 to 15 m3/s [20].

To analyze the data from this experiment, Godfrey & Frederick made an initial analysis of the field data, and Thackston, Hays & Krenkel then carried out a detailed analysis of the possible theoretical alternatives to calculate the Longitudinal Coefficient of Dispersion, since the curves obtained experimentally, they showed some bias (of the Pearson-III type), and the conventional methods of the time did not allow adequate accuracy. For this reason, it was preferred to use the Moments method, which does not recognize the so-called "convective period" (recognized by most other methods), which prevented its application in the early phase of the tracer's evolution. This method only requires that the velocity be approximately constant [21].

To compare the results of the classical Method of Moments and the Method based on the application of the State Function, presented in this Article, the experiment in the Cooper Creek River, VA is analyzed. USA, previously documented. Thus, pouring tracer at an "upstream" point, and measuring the passage of the tracer "downstream", at X1≈2.40 Km, and X≈4.10 Km. The data were shown in Table 1.

Table 1: Concentration data. Source: Prepared by the authors based on (McCutcheon & Martin, 1999). Source: Prepared by the authors based on (McCutcheon & Martin, 1999).

Tiempo (s)	Concentración 1 (ppb)	Concentración 2 (ppb)
0		
600		
1200		
1800	0,02	
2400	3,92	
3000	39,5	
3600	97,3	0,01
4200	**107**	**0,41**
4800	71,9	5,11
5400	34,6	24,1
6000	13,2	57,1
6600	**4,24**	**82**
7200	1,2	80,9
7800	0,31	59,8
8400	0,01	35,3
9000		17,4
9600		7,4
10200		2,79
10800		0,95
11400		0,3
12000		0,09
12600		0,02
13200		0,01
13800		
14400		
15000		

Source: Authors, (2021).

The next Figure 17 presents the graphing of the sequential curves corresponding to the data in Table 1.

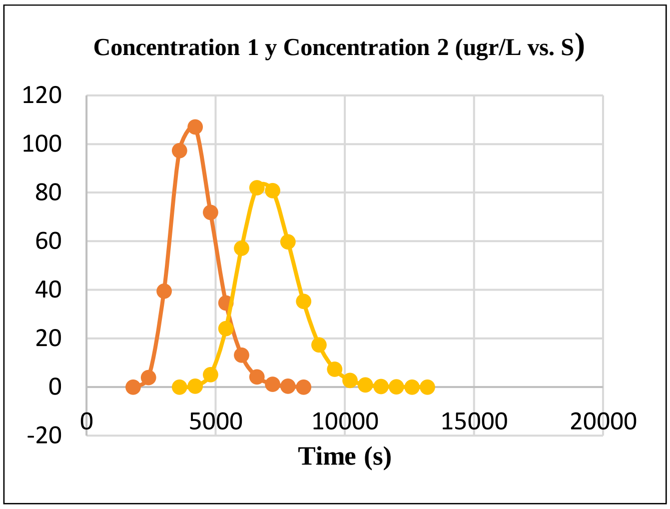

Figure 17: Plotting of the tracer data over time. Source: Authors' elaboration.
Source: Authors, (2021).

The statistical technique of Moments, operates under the assumption that the flared tracer curve can be assimilated to a Gaussian curve, in an approximate way, and thus the Longitudinal Dispersion Coefficient, E.

$$E \approx 0.5\left(\frac{d\sigma_x^2}{dt}\right) \tag{27}$$

As the discrete experimental data are normally available as a function of time, the above equation can be transformed as follows:

$$E \approx \frac{U^2}{2}\left[\frac{\sigma_{t2}^2 - \sigma_{t1}^2}{<t_2>-<t_1>}\right] \tag{28}$$

That is, the reason for the differences in the temporal variances at the two measurement points, and the mean times at those points.

Properly manipulating the experimental data and applying the corresponding equations to this method, we have for the two points considered, both the centroid times of the curves, as well as the variances. For these calculations, usual statistical formulas are applied [22].

$$tc1 = \frac{\int t{*}Cdt}{\int Cdt} = \frac{26298\, min{*}ug/l}{373{,}2\, ug/l} \approx 70{,}47\, min \tag{29}$$

$$tc2 = \frac{\int t{*}Cdt}{\int Cdt} = \frac{45581\, min{*}ug/l}{373{,}7\, ug/l} \approx 118{,}8\, min \tag{30}$$

And:

$$\sigma t1^2 = \frac{\int t^2{*}Cdt}{\int Cdt} - t_c^2 = \frac{1926000\, m2{*}\frac{ug}{l}}{373{,}2\frac{ug}{l}} - (70{,}47\ \mathrm{min})^2 \approx 195{,}0\, min^2 \tag{31}$$

$$\sigma t2^2 = \frac{\int t^2{*}Cdt}{\int Cdt} - t_c^2 = \frac{5537766\, m2{*}\frac{ug}{l}}{373{,}7\,\frac{ug}{l}} - (118{,}2\, min)^2 \approx 319{,}8\, min^2 \tag{32}$$

Now, the average flow velocity is calculated in this method by the following formula:

$$U = \frac{X_2 - X_1}{tc_2 - tc_1} \approx \frac{(4100-2400)m}{(118{,}8-70{,}47)min} \approx 35{,}17\ m/min \qquad (33)$$

Therefore, the Longitudinal Coefficient of dispersion in this case is:

$$E = \frac{U^2}{2} * \frac{(\sigma_{t2}^2 - \sigma_{t1}^2)}{(t_2 - t_1)} \approx \frac{(35{,}17\ m/min)^2}{(118{,}8-70{,}47)min} * (319{,}8 - 195)m2 \approx 1595\ m^2/min \qquad (34)$$

Transforming this expression from minutes to seconds we have:

$$E \approx 27{,}0\ m^2/s \qquad (35)$$

This is then the average value of the Longitudinal Dispersion Coefficient in the section studied, obtained with the classic statistical method of Moments.

The next step is to apply the method that includes the State function and compare the results with the previous data. This analysis is part based on the following Figure 18.

For this figure, tv1 and tv2 are the times for the peak of each distribution, and tpp1 and tpp2 are the times of the first particles of each distribution. Likewise, δ´1 and δ´2 are the standard deviations of each distribution in time, multiplied by two.

For the concrete calculations of the State Function theory, we have the following approximate formulas, based on the properties of the Gaussian function.

$$\Phi(t) \approx (\delta')/tv \qquad (36)$$

It is now possible to calculate the values of the State Functions at each time of interest.

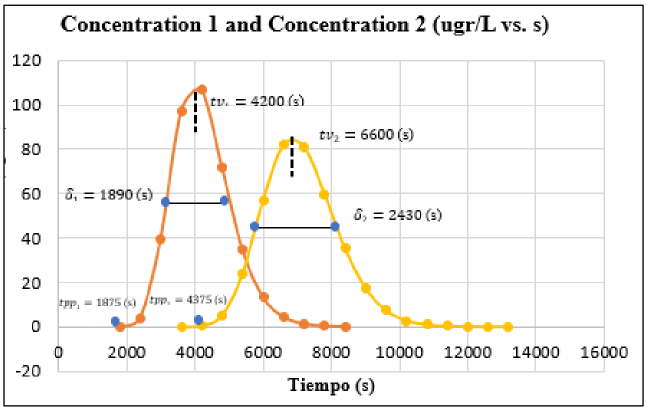

Figure 18: Data for corresponding calculations.
Source: Authors, (2021).

$$\Phi_1(4200) = \frac{\delta'_1}{tv_1} = \frac{1890}{4200} = 0{,}45 \qquad (37)$$

$$\Phi_2(6600) = \frac{\delta'_2}{tv_2} = \frac{2430}{6600} = 0{,}37 \qquad (38)$$

Note that the available documentation of this experiment does not report neither the mass nor the flow, data that are needed to model tracer curves, equation (24). To solve this fault, the ratio "M / Q" is calculated. For the first curve:

Cp1~107.0 (ugr/L), Φ1 ~0.45 and ***tv1~4200 s***

$$(\frac{M}{Q})1 \approx 107\ \left(\frac{ugr}{l}\right) * 0{,}45 * 4200 * 1{,}16 \approx 234587 \qquad (39)$$

Curve 1 modeling:

With these data, the first tracer curve can be modeled, applying equation (24). The blue curve is the experimental data, while the built model is the green curve. Figure 19.

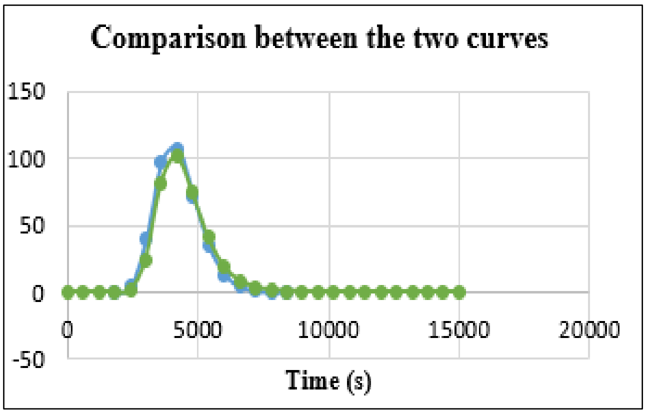

Figure 19: Experimental curve 1 and model with Φ (t).
Source: Authors, (2021).

Now, the slight lag observed in the modeling of the experiment in curve 1 can be improved with changes in the time of the peak, and in the data of the state function, for that specific point, like this:

Cp1~108.9 ug*/L*, ***Φ1~0.41***, *and* ***tv1~4100 s****.*

These changes are included in equation (24), which describes the Fickian curve 1, shown below. Figure 20:

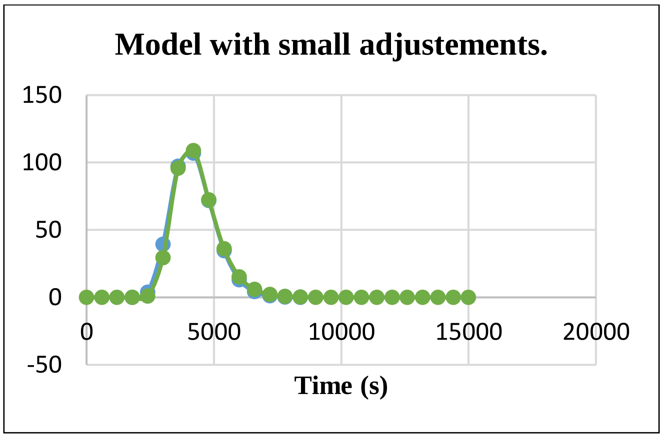

Figure 20: New modelling of first curve with small changes.
Source: Authors, (2021).

Curve 2 modeling:

We now proceed to model the curve at point 2, considering the corresponding data:

Cp~82.0 (ugr/l), ***Φ~0.37***, and ***tv~6600 s.***

For this new curve, the ratio "M / Q" must be recalculated, from the attenuation factor that is valid there. For this new curve, the ratio “M/Q” must be recalculated, from the attenuation factor that is valid there.

$$(\frac{M}{Q})2 \approx 82\ \left(\frac{ugr}{l}\right) * 0{,}37 * 6600 * 1{,}16 \approx 232283 \qquad (40)$$

This value for the second curve is virtually the same as that calculated for the first curve, indicating good precision for the implicit value of the flow rate (whatever it is). For the modeling of curve 2, the procedure used in curve 1 is repeated. Figure 21.

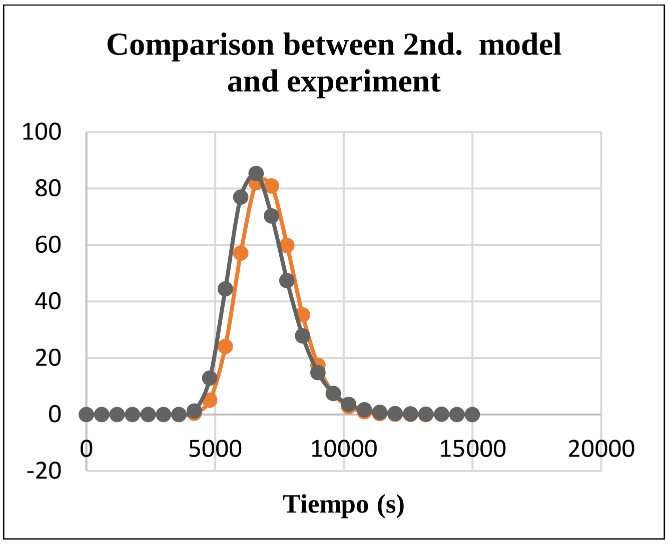

Figure 21: Experimental curve and model with Φ (t).
Source: Authors, (2021).

Again, it is seen that between the theoretical model (gray) and the experimental data (orange) there is an evident lag between the curves. Now, if the data in table 1 is analyzed in detail, it can be observed that in this area of the peak (of abrupt variation), the temporal separation of the sequential measurements is "greater" than the required temporal resolution. So, the "true" time of the peak (for the model) is a little further to the right in time. We then have the following characteristic set:

Cp2~ 82.0 (ugr/L) , ***Φ2~0.344***, and ***tv**~**6650 s***

With these values in equation (24), we have that quite coincident curves are obtained. Figure 22.

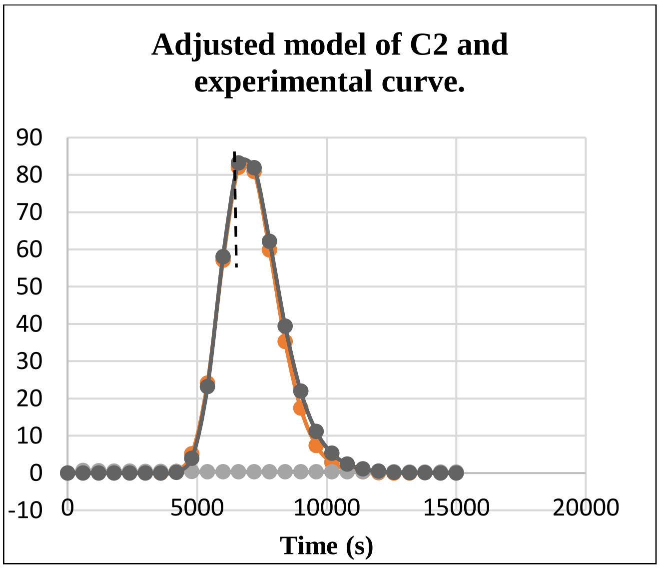

Figure 22: Refined curve with better data.
Source: Authors, (2021).

From the "optimal" data (which corresponds to the curves in Figures 20 and 22), previously established for the section under study, the value of the Longitudinal Dispersion Coefficient is calculated and compared with the original data established by the Method of Moments.

Curve 1:

The optimal data set is:

Cp1~108.9 ug/**L*, ***Φ1~0.41, *and* ***tv1~4100 s**.*

Therefore:

$$E1 \approx \frac{\varphi^2 * U^2 * \beta * tv}{2} \approx \frac{0{,}41^2 * 0{,}59^2 * 0{,}214 * 4100}{2} \approx 25{,}7\ m2/s \tag{41}$$

Curve 2:

The optimal data set is:

Cp2~ 82.0 (ugr/L) , ***Φ2~0.344***, and ***tv**~**6650 s***

Therefore:

$$E2 \approx \frac{\varphi^2 * U^2 * \beta * tv}{2} \approx \frac{0.344^2 * 0{,}62^2 * 0{,}214 * 6650}{2} \approx 32.4\ \ m2/s \tag{42}$$

An average value for the two curves 1 and 2 is:

$$< E > \approx \frac{25.7+32.4}{2} \approx 26{,}7\ m2/s \tag{43}$$

As can be seen, the value of the Longitudinal Dispersion Coefficient calculated with the State Function Method is remarkably close to that calculated with the classical Method of Moments, with a relative error of 1%. The State Function Method works with the velocity of the peak of the concentration and does not recognize an initial period in which Fickian physical theories cannot be applied for its interpretation. Nor does it need the concept of "Centroid" (difficult to calculate) which is explained in a natural way, because of the unavailability of mass for dispersion, which is measured by the decaying values of the State Function.

It also offers a direct explanation of the skew characteristic of these curves. Finally, calculating the peak velocities for the two measurement points, U1≈0.59 m / s and U2≈0.62 m / s, the established by L. Leopold [23] is verified in that the average velocities of a natural channel in "Dynamic equilibrium" are approximately constant, as already explained, ensuring in a certain way, the accuracy of the Moments method.

IV. RESULTS, DISCUSSIONS AND RECOMMENDATIONS

1 - As analyzed in detail in this Article, the "linear" nature of turbulence responds to a relatively small value of the notable factor (W/RT), which defines the "fluidity" of liquid water at room temperature and facilitates attenuation. of speed fluctuations. This condition allows the application of Prigogine's theorem of the minimum entropy production, and therefore of the fulfillment of the "equiprobability" in the system.

In this circumstance, what is described in Figure 4, about the statistical constancy of the mass transfer between points of the system, and consequently of a "constant" average flow velocity along the course of the channel, is approximately fulfilled. The real degree of compliance with this condition is reflected in a lower or greater absolute error, equations (6) and (7).

2 - The dynamics of the tracers in turbulent flows is not independent of the turbulence itself. With the injection of the tracer to the flow, the local thermodynamic condition of the same is disturbed, since the plume carries a certain amount of Free Energy, which is spent by irreversible effects, as the plume advances in time and space, as in Figure 13.

3 - The above indicates that said irreversible evolution of the tracer in turbulent flow is governed by the general laws of

thermodynamics, and therefore it is essential to determine a "State function" that describes said evolution. The authors have presented a model of such a function in this regard. This function is applied to a specific case of a tracer experiment, taken from the technical literature, and is compared with the classical numerical results of the Statistical Moments method. The comparison between the two methods is completely satisfactory, supporting the theoretical assumptions on which the new method was based.

4 - A hardware-software tracer device is presented that operates in "real time" and incorporates the new tracer evolution state function.

5 - Further research should determine the values of the constants "a" and "b" of the equations that link the state function and the production of entropy.

V. AUTHOR'S CONTRIBUTION

Conceptualization: Alfredo Jose Constain, Gina Peña Olarte and Carlos Peña Guzman.
Methodology: Alfredo Jose Constain, Gina Peña Olarte and Carlos Peña Guzman.
Investigation: Alfredo Jose Constain, Gina Peña Olarte and Carlos Peña Guzman.
Discussion of results: Alfredo Jose Constain, Gina Peña Olarte and Carlos Peña Guzman.
Writing – Original Draft: Alfredo Jose Constain, Gina Peña Olarte and Carlos Peña Guzman.
Writing – Review and Editing: Alfredo Jose Constain, Gina Peña Olarte and Carlos Peña Guzman.
Resources: Alfredo Jose Constain, Gina Peña Olarte and Carlos Peña Guzman.
Supervision: Alfredo Jose Constain, Gina Peña Olarte and Carlos Peña Guzman.
Approval of the final text: Alfredo Jose Constain, Gina Peña Olarte and Carlos Peña Guzman.

VI. ACKNOWLEDGMENTS

Our thanks to the "Fluvia" company and to the "Universidad de la Salle", in Bogota, Colombia, for their permanent support to these research tasks.

VII. REFERENCES

[1] P. W. Anderson, «Physics: the opening to complexity.», Proc. Natl. Acad. Sci. U. S. A., vol. 92, n.o 15, pp. 6653-6654, jul. 1995.

[2] I. Prigogine and G. Nicolis, "La estructura de lo complejo". Alianza Editorial. Madrid, 1987.

[3] D. Kondepudi and I. Prigogine, "Modern Thermodynamics". Wiley, USA, 1996.

[4] L.B. Leopold and W. Langbein, "The concept of entropy in landscape evolution". USGS Paper 502-A, 1962.

[5] I. Prigogine, "The end of certainty". Free Press, USA. 1997.

[6] I. Prigogine, "Las leyes del caos". Critica, Barcelona, 1997.

[7] R. Penrose, "The Cycles of time". Random House, Barcelona.2010.

[8] D. Kondepudi and I. Prigogine I., Ibid, 1996.

[9] J. Frenkel, "Kinetic theory of liquids". Dover, USA, 1955.

[10] A. Christofoletti, "Geomofologia fluvial". Edgard Blucher, Sao Paulo. 1981.

[11] T. Ochoa, "Hidraulica de rios y procesos morfológicos". ECOE Ediciones, Bogota, 2011.

[12] A.Constain, C. Peña-Guzman and D. Mesa, "Equivalence of local and general mass transport rates in natural beds in dynamic equilibrium", Aqualac, Montevideo, 2015. V7. 1-02.

[13] A. Constaín and R. Lemos, «Una ecuacion de la velocidad media del flujo en regimen no uniforme, su relacion con el fenomeno de dispersion como funcion del tiempo y su aplicacion a los estudios de calidad de agua», Ing. Civ., vol. 164, pp. 114-135, 2011.

[14] A. Constain, «Definición y análisis de una función de evolución de solutos dispersivos en flujos naturales», Dyna, vol. 175, pp. 173-181, 2012.

[15] H.B. Fischer "Dispersion predictions in Natural streams". Journal of Sanitary Engineering división, ASCE, october, 1968.

[16] H.B. Fischer. "Longitudinal dispersion in laboratoryand natural streams". Report No. KH-R-12, June 1966, USA.

[17] T. Makela. and A. Annila, "Natural patterns of energy dispersal". Physics of life review. 7 (2010)

[18] R Godfrey. and B. Frederick, "Stream dispersión at selected sites". USGS 433-K Paper. 1070.

[19] L. B Leopold, «Downstream change of velocity in rivers», Am. J. Sci., vol. 251, n.o 8, pp. 606-624, ago. 1953.

[20] J.L. Martin and S.C McCutcheon, "Hydrodynamics and transport for wáter quality modeling". Lewis. Boca ratón. 1999.

[21] H.B. Fischer. Ibid. 1966

[22] J.L Martin and S.C McCutcheon. ibid. 1999.

[23] L. B. Leopold. Ibid 1953.